Emergent Materials
https://doi.org/10.1007/s42247-024-00711-3

ORIGINAL ARTICLE

3D-printed polylactic acid (PLA)/polymethyl silsesquioxane (PMSQ)-based scaffolds coated with vitamin E microparticles for the application of wound healing

Nasma Anjrini[1,2] · Hatice Karabulut[1,3] · Songul Ulag[1,4] · Hasan Ege[1,5] · Cansu Noberi[1,6] · Ecem Dogan[1] · Ali Sahin[7,8] · Oguzhan Gunduz[1]

Received: 11 June 2023 / Accepted: 12 April 2024

Abstract
Skin is part of the integumentary and excretory system, which helps protect the body against infections. The skin should be properly treated when it gets injured, which requires a long healing process. In this study, 15% (w/v) polylactic acid (PLA) and 1 and 2% (w/v) polymethylsilsesquioxane (PMSQ) scaffolds were fabricated using 3D printing technology, and the surfaces of each scaffold were coated with 5% ethylcellulose (EC)/vitamin E microparticles using the electrospray method. The morphologies of the scaffolds were characterized using a scanning electron microscope (SEM), and results showed that the pore sizes of the scaffolds ranged from 136 to 265 µm. The vitamin E was completely released from the scaffolds within 5 h. MTT test was performed with fibroblast cells and results proved the biocompatibility of the scaffolds. These findings showed that the scaffolds may have good potential as a wound dressing material. The biodegradation test was performed in in vitro conditions and results showed that the surface coating with 5% EC/vitamin E microparticles on the 15% PLA/2% PMSQ scaffolds increased the degradation rate of the scaffolds.

Keywords Electrospray · Microparticles · PLA · PMSQ · Vitamin E · Wound healing · 3D printing

1 Introduction

Skin wounds are injuries resulting from trauma and mechanical tears to skin tissue [1]. This can cause blood loss and maybe shock [2]. In this case, rapid hemostasis is important since the recovery of damaged skin after hemostasis is a slow and complex process [3]. Wound healing involves several stages, including inflammation, tissue repair, and tissue reconstruction [4]. When inflammation forms in a wound, the body's immune system responds by secreting white blood cells to the affected area to protect against infection and initiate the tissue repair process. This can cause swelling, redness, and warmth at the wound site. In the tissue repair phase, new cells called fibroblasts are produced and begin to release the collagen protein that helps form new tissue. The wound begins to fill with new tissue and the wound area begins to close by the edges of the wound. Various factors, such as the size and depth of the wound, the presence of infection, and the individual's general health status, can affect the wound healing process. Thus, medications or other treatments may be necessary to promote healing. Another factor that inhibits the healing process of the

✉ Oguzhan Gunduz
oguzhan@marmara.edu.tr

1 Center for Nanotechnology & Biomaterials Application and Research (NBUAM), Marmara University, Istanbul, Turkey

2 Department of Bioengineering, Faculty of Natural Sciences and Engineering, Uskudar University, Istanbul, Turkey

3 Institute of Pure and Applied Sciences, Metallurgical and Materials Engineering, Marmara University, Istanbul, Turkey

4 Health Institutes of Türkiye (TUSEB), Istanbul, Turkey

5 Department of Physiology, Institute of Health Sciences, Istanbul University-Cerrahpasa, Istanbul, Turkey

6 Department of Mechatronics Engineering, Faculty of Engineering and Architecture, Istanbul Gelisim University, Istanbul, Turkey

7 Department of Biochemistry, Faculty of Medicine, Marmara University, Istanbul, Turkey

8 Genetic and Metabolic Diseases Research and Investigation Center (GEMHAM), Marmara University, Istanbul, Turkey

Published online: 15 May 2024

wound is high levels of reactive oxygen species (ROS) [5]. At low concentration levels of ROS, they will act as a messenger for migrating cells, accelerating the healing process and angiogenesis [6]. Today, traditional dressing materials such as gauze are widely used in clinical practice for wound healing. However, these materials exhibit weak hemostatic effects and may cause problems such as tissue adhesions when in contact with the wound for a long time [7]. These disadvantages have increased the interest in new wound dressing materials such as 3D scaffolds, hydrogels, films, nanofibers, and sponges [8, 9].

In recent years, 3D bioprinting technology has emerged as a new technological approach for producing layer-by-layer complex biobased structures with cell-containing bioinks [10, 11]. In tissue engineering applications, 3D printing has a special function in creating scaffolds. These scaffolds' high surface area and small hole diameters are necessary for optimal cellular interactions and the development of new functional tissues [12]. The utilization of 3D printing technology presents a benefit in the creation of safe, durable, and economical implantable scaffolds by enabling the production of intricate geometries with uniform cell distributions [13]. Therefore, several criteria, including the intended shape, size, porosity, mechanical strength, drug loading, release profile, biocompatibility, and cost-effectiveness of the scaffold, influence the decision to choose 3D printing over gel formulation for the scaffold drug delivery system [14].

Electrospraying, also known as electrodynamic spraying, can produce tiny droplets with submicron sizes after employing an electric field [15]. The electrostatic force is utilized to break the surface tension of the charged liquid in a syringe [16]. Nanoparticles or microparticles produced by the electrospraying method are loaded with drugs or supplements known for their healing properties or effects on infections and are used as drug delivery vehicles or drug release platforms [17].

PLA has desired properties such as being biocompatible, biodegradable, and mechanical strength and it provides desirable controlled release of functional drugs and supplements [18]. PMSQ is a material that has been used widely in skin care products and cosmetics. It has good mechanical properties with a large elastic module range (8.500–10.000 MPa). It has an organic–inorganic nature that provides it with thermal stability. Also, its elasticity in addition to its chemical nature serves the goal of using it on the skin (https://www.wacker.com/h/en-us/silicone-resins/silicone-resins-inci/belsil-PMSQ-powder/p/000009684.).

Vitamin E is a fat-soluble supplement used as a microparticle because of its ability to improve skin healing through its chemical and physical stabilities. Its physical stability is provided by adhesive films which lead to the occlusive effect that provides penetration of the vitamin on the skin [19]. Ethyl cellulose (EC) is used as a barrier to deliver vitamin E microparticles and assist the release process on the skin due to its hydrophobicity, lipophilicity, and non-toxicity properties [20].

In this study, 3D-printed scaffolds were produced using polylactic acid (PLA) and polymethylsilsesquixane (PMSQ) polymers. The fabricated PLA/PMSQ 3D-printed scaffolds were coated with EC/vitamin E microparticles by electrospray method. The particles have drawn a lot of interest from the biomedical research community and offer a viable platform for cutting-edge medication delivery systems. Owing to these intrinsic characteristics, coating nanoparticles to the scaffold appears to be a far better and unique method than merely combining them with the scaffold matrix. Therefore, in his study, we used the electrospray method to coat the 5% EC/vitamin E microparticles onto 3D-printed 15% PLA/2% PMSQ scaffolds, aiming to evaluate their potential as therapeutic agents for wound healing.

2 Materials & Method

2.1 Materials

Poly (lactic acid) (PLA) 4060D (MW ~ 92 kDa) as granule form was obtained from NatureWorks LLC, Minnetonka. Polymethylsilsesquioxane (PMSQ) polymer (MW = 7465 g/mol), in powder form, was purchased from Wacker Chemie AG, GMBH (Burghausen, Germany) under BELSIL® PMS-MK trademark name. Ethyl cellulose (viscosity 46 cP, 5% in toluene/ethanol) was purchased from Sigma-Aldrich (St Louis, MO, USA). Vitamin E (D-α-Tocopherol) was purchased from Kocak Farma, Turkey, and as solvents chloroform was purchased from Merck, Germany, and absolute ethanol was purchased from Isolab. Phosphate buffer saline (PBS) (pH 7.4) was supplied from Chembio (Istanbul, Turkey).

2.2 Preparation of each solutions

Firstly, 15% (w/v) PLA polymer solution was prepared dissolving 1.5 g of PLA in 10 mL of chloroform for 1 h at 500 rpm. Then, PMSQ polymer was added into homogenous 15% PLA solutions separately at concentrations of 1% and 2% (w/v) and mixed for an extra 30 min on the magnetic stirrer. Each solution was prepared at room temperature (25 ± 2 ℃) and transferred into a 10 mL plastic sterile syringe. For microparticle production, EC was dissolved in ethanol at a concentration of 5% (w/v). After 5% EC was completely dissolved in a magnetic stirrer at 700 rpm for one hour, 1 tablet of vitamin E was added to the solution. The EC/vitE solutions were mixed using a high-speed homogenizer (8000 rpm) for 2 min to obtain homogeneous solutions.

2.3 Fabrication of the 3D-printed scaffolds

The scaffolds were fabricated using an extrusion-based 3D bioprinter (Hyrel 3D, SDS-5 Extruder, GA, USA). The 15% PLA and 15% PLA/(1–2) % PMSQ solutions in a 10 mL plastic sterile syringe were connected to the printer using a plastic needle that has a 0.2 mm diameter. The scaffolds were designed as squares in dimensions 20 mm × 20 mm using the solidworks program and converted to G-code (Fig. 1). Printing process parameters were controlled using solidworks and scaffolds were printed as 6 layers in total, printing speed of 10 mm/s, flow rate of 1 ml/h, and at room temperature (25 ± 2 ℃).

2.4 Electrospraying of microparticles on the 3D-printed scaffolds

The microparticles were fabricated using a laboratory-scale electrospray machine (NS24, InovensoCo, Turkey). Firstly, 5% EC/vitamin E solution was placed into a 10 mL plastic sterile syringe and connected to a syringe pump (NE-300, New Era Pump Inc., Toledo, OH, USA). The stainless-steel needle which has a 0.3 mm inner and 0.8 mm outer needle was used. The flow rate was adjusted to 13 µL/min, the voltage value was 23 kV and the distance between the needle tip and grounded collector was set to 10 cm. The 5% EC/vitamin E microparticles were sprayed only on the surface of 15% PLA/2% PMSQ scaffolds (Fig. 1).

2.5 Morphological analysis of the scaffolds

The morphology of each scaffold was analyzed using scanning electron microscopy (SEM, EVA MA 10, ZEISS) after coating the surface of the scaffolds with gold under a coating machine (Quorum SC7620, USA) for 10 s. The average pore sizes and their distributions were investigated using image software (Olympus AnalySIS, Waltham, MA, USA).

2.6 Thermal characterization of the scaffolds

The thermal properties of each scaffold were investigated using differential scanning calorimetry (DSC-60 Plus model, Shimadzu, Kyoto, Japan) in a temperature range (25–200° C) at a rate of 25° C/min.

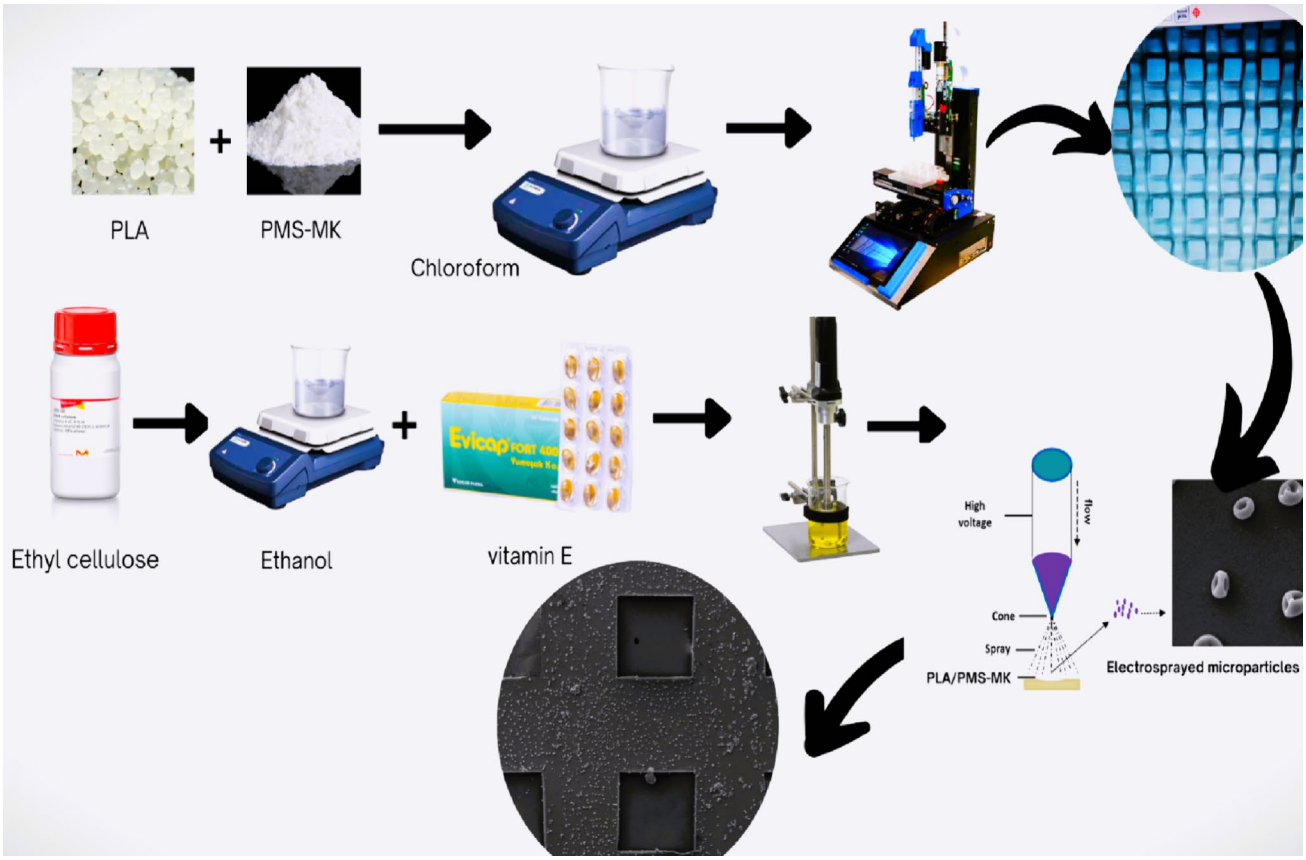

Fig. 1 Methodology of the experiment

2.7 Chemical analysis of the scaffolds

The chemical properties and bonds of each scaffold were obtained using fourier transform infrared spectroscopy (FTIR, 4700 Jasco, Japan), which was used with (4000–400 cm^{-1}) scanning wavelength range and (4 cm^{-1}) resolution.

2.8 Mechanical properties of the scaffolds

The tensile strength and strain properties of each scaffold were analyzed using a tensile test machine (EZ-X model, Shimadzu, Kyoto, Japan). Firstly, the thickness of each sample was measured with a digital micrometer (Mitutoyo MTI Corp., USA). The speed of the tensile testing machine was adjusted to 5 mm/min and the mechanical properties were tested at room temperature. The force was fixed to the value of 0.1 kN. The mechanical properties of each scaffold were performed by testing three samples of each same scaffold. The scaffolds were placed directly between the jaws of the device to measure the tensile strength and strain values of the scaffolds under this force.

2.9 Biodegradation test

The degradation behavior of the scaffolds was investigated for 5 days. The initial weight of scaffolds (W_0) was measured on the first day, then scaffolds were placed in 1 mL of phosphate-buffered saline (PBS, pH: 7.4) and were put on a thermal shaker (BIOSAN TS-100C) at 37 ℃ and 400 rpm. After every 24 h, the scaffolds were removed from the PBS solution and dried for 24 h in the incubator at 37 ℃, The dried weight of the scaffolds was measured and 1 mL of fresh PBS solution was added after each measurement.

$$D_i = \frac{W_0 - W_D}{W_0} * 100\% \quad (1)$$

In this Eq. (1), W_0 is the initial weight, W_D is the dried weight, and D_i is the degradation ratio.

2.10 In vitro drug release analysis of vitamin E

The release behaviors of vitamin E from 15% PLA/2% PMSQ scaffolds were performed after immersing 5 mg of the scaffold in 1 mL of phosphate buffer solution (PBS, pH: 7.4) in a thermal shaker (BIOSAN TS-100C) at 37 ℃ and 400 rpm. Absorbance values were measured using a UV spectrophotometer (Shimadzu- UV-1280, Japan). After each measurement, fresh PBS solution was added to scaffolds and left again on the thermal shaker for the specific time interval. The absorbance wavelength points of vitamin E were between (232–238 nm). Five different vitamin E concentrations were prepared as (0.2, 0.4, 0.6, 0.8, and 1.0 µg/ml), and measured a using UV spectrophotometer (Shimadzu- UV-1280, Japan). Then the calibration curve was plotted at wavelength ranging between 200 and 340 nm.

2.11 Biocompatibility analysis using MTT assay

Firstly, fabricated scaffolds were prepared by being sterilized overnight under UV light in 96well plates, then it was incubated in DMEM growth medium with 10% of Fetal bovine serum (FBS) and 0.1 mg/ml penicillin/streptomycin at 37 °C with 5% CO_2 atmosphere for one hour. After incubation, fibroblast cells were seeded with the density of 50000 cells/scaffold on the scaffolds in 96 well plates same as the standard cell culture procedure. Cytotoxicity detection kit (MTT from Glentham Life Sciences) was used to investigate cellular metabolic activity as an indicator of cell viability, proliferation, and cytotoxicity to obtain the biocompatibility of the scaffolds after 1st, 3rd, and 7th days of incubation. Elisa reader (Perkin Elmer, Enspire) was used to obtain the absorbance values at 560 nm wavelength. The measurements were repeated three times and the mean values were taken as the result. SEM images were taken to investigate the cellular morphology of fibroblast cells on the scaffolds. After 3 days, the growth medium was dispensed, and scaffolds were treated with 4% glutaraldehyde (Sigma Aldrich), then dried using serial dilution and air dried.

3 Results & discussions

3.1 Morphological analysis by SEM

The morphology of each scaffold and its pore structures were analyzed using an SEM, and the results are shown in Fig. 2. According to SEM images, the lowest mean pore size was observed for 15% PLA scaffold and found to be 135.47 ± 13.71 µm (Fig. 2a). With the addition of PMSQ to the 15% PLA, the mean pore size of the scaffold increased. Figure 2(b) shows the SEM images and pore size distribution of the 15% PLA/2% PMSQ scaffold, and the mean pore size value was found to be 265.42 ± 16.91 µm. However, the mean pore size of the 15% PLA/2% PMSQ scaffold decreased to a value of 203.44 ± 7.79 µm when its surface was coated with EC/vitamin E microparticles (Fig. 2c). Based on the SEM images, it is noticeable that the addition of PMSQ increased the pore size value compared to the 15% PLA scaffold. On the other hand, after coating the surface of the 15% PLA/2% PMSQ scaffold with EC/vitamin E microparticles the mean pore size decreased when

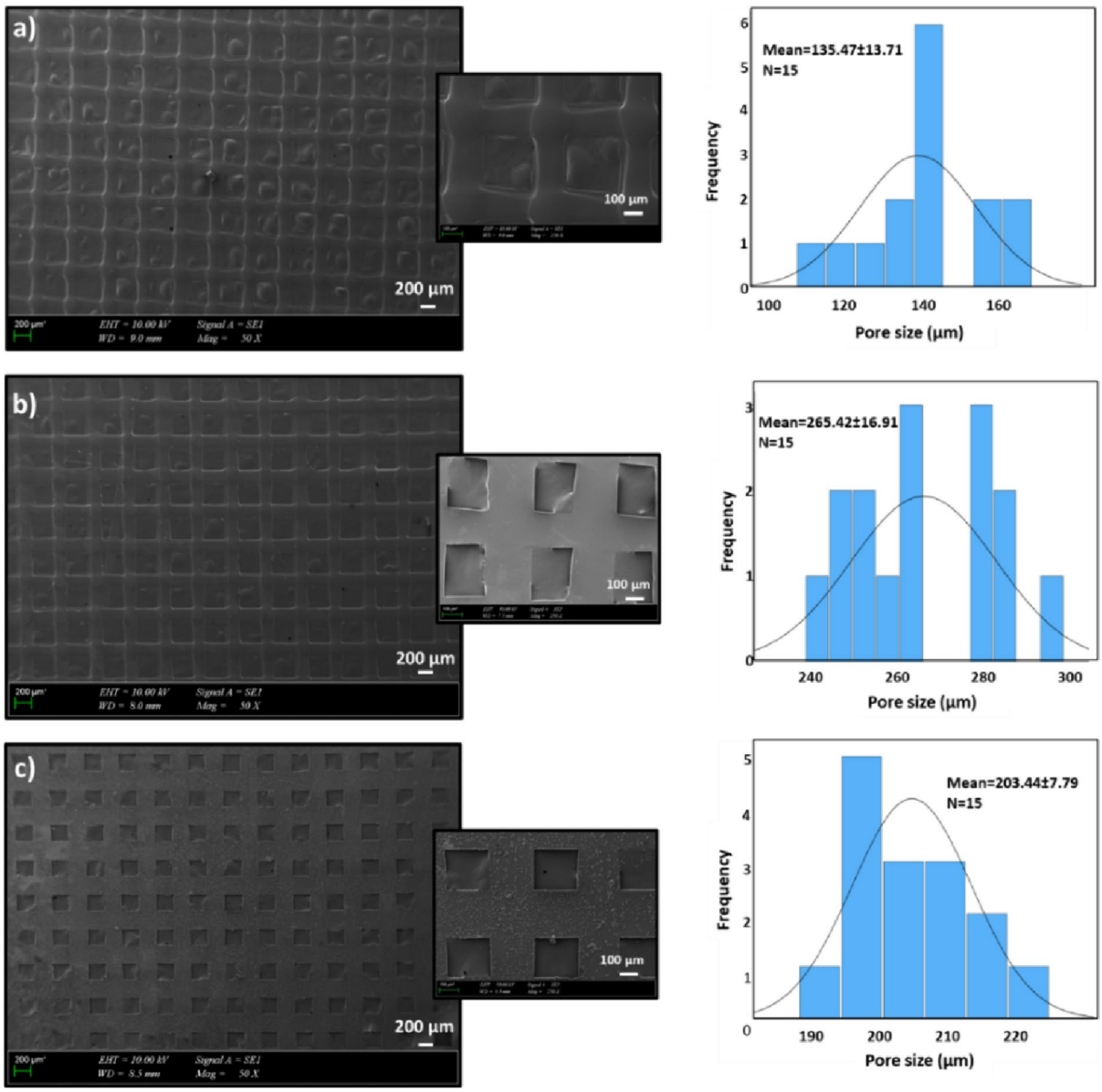

Fig. 2 SEM images of 15% PLA (**a**), 15% PLA/2% PMSQ (**b**), and 15% PLA/2% PMSQ coated with vitamin E (**c**) and graphs of their pore size distributions

compared to 15% PLA/2% PMSQ scaffold as its surface area was covered with microparticles which has been sprayed homogeneously over the scaffolds. Additionally, all scaffolds were easily printed without any clogging problems, and the pores of each scaffold were visible. If the pore size of the scaffold is less than 325 µm, cells can attach, proliferate, and differentiate since it will be easier to imitate the extracellular matrix. Therefore, we can say that the fabricated 3D-printed scaffolds can easily provide a suitable environment for cell attachment, migration, adhesion, and differentiation [21].

3.2 Thermal characterization of each scaffold

The thermal analysis was performed using differential scanning calorimetry to investigate the effect of heat and chemical interaction that lead to glass transition, melting, and crystallization on the fabricated scaffolds. Figure 3(a) represents the DSC curve of the 15% PLA/2% PMSQ scaffold coated with vitamin E which showed endothermic peaks at 70.03 ℃ and 151.64 ℃ due to the glass transition of PLA at 70 ℃ and melting point of PLA at 150 ℃ [22, 23]. Additionally, PMSQ addition might have improved

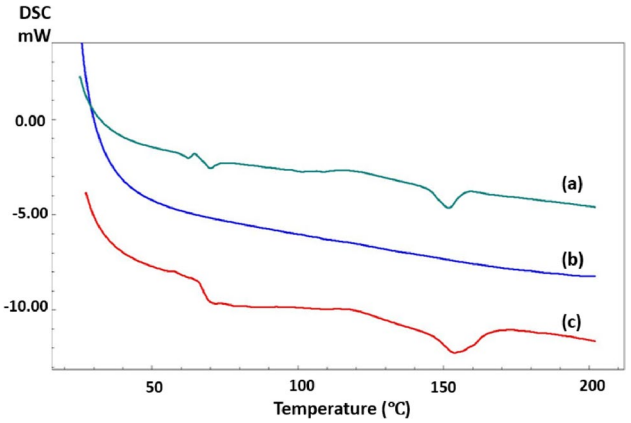

Fig. 3 DSC curves of the 15% PLA/2% PMSQ scaffold coated with vitamin E (**a**), vitamin E (**b**), and 15% PLA/2% PMSQ scaffold (**c**)

the thermal characteristics of PLA-based scaffolds since a very small change was observed in the melting point of PLA when compared to the study by Croitoru et. al. [23]. Figure 3(b) represents the DSC curve of vitamin E which did not show any peaks. Figure 3(c) represents the DSC curve of a 15% PLA/2% PMSQ-based scaffold that showed endothermic peaks at 65.99 ℃ and 153.86 ℃. These results indicated that the melting temperatures of both 15% PLA/2% PMSQ and 15% PLA/2% PMSQ scaffolds coated with 5% EC/vitamin E microparticles were close. However, the 15% PLA/2% PMSQ scaffold coated with vitamin E microparticles showed similar thermal behavior to the 15% PLA/2% PMSQ scaffolds.

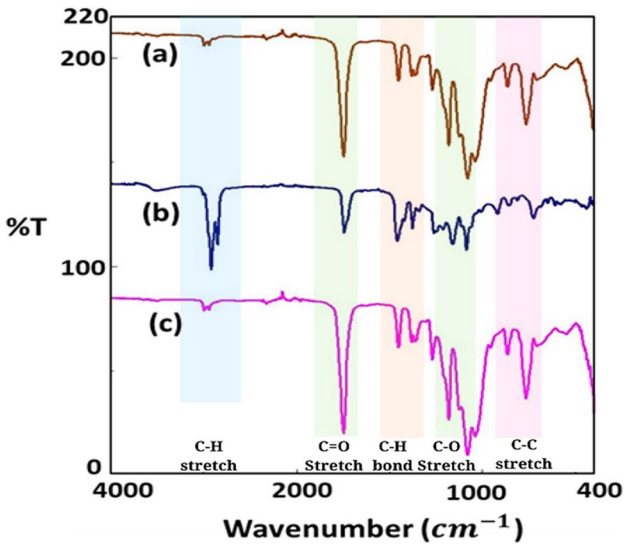

Fig. 4 FTIR spectrums of 15% PLA/2% PMSQ scaffold coated with vitamin E (**a**), vitamin E (**b**), and 15% PLA / 2% PMSQ (**c**)

3.3 Chemical analysis

For chemical analysis and the detection of heterogeneity in scaffolds, FTIR analysis was performed, and Fig. 4 represents the FTIR spectra of each scaffold and vitamin E. Figure 4(a) shows the spectrum of the 15% PLA/2% PMSQ scaffold coated with vitamin E. There was a peak at 1747.19 cm^{-1} which represents C = O stretching, and other peaks were observed at 1452.14 cm^{-1}, 1382.71 cm^{-1}, 1359.57 cm^{-1}, 1268.93 cm^{-1} which represent C-H bonding of PLA [24]. The peaks at 1180.22 cm^{-1}, 1124.30 cm^{-1},10 79.94 cm^{-1},1039.44 cm^{-1} which represent C-O stretching, and peaks at 865.88 cm^{-1}, 765.60 cm^{-1}, 707.75 cm^{-1} represents C–C stretching [25, 26]. Figure 4(b) shows the pure vitamin E spectrum, which showed peaks at 2921.63 cm^{-1}, and 2852.20 cm^{-1} which presents C-H stretching, and a peak at 1745.26 cm^{-1} which presents C = O stretching. Other peaks at 1457.92 cm^{-1}, 1421.28 cm^{-1}, and 1340.28 cm^{-1} are related to C-H bonding. Additionally, there were peaks at 1159.01 cm^{-1} and 1006.66 cm^{-1} which represent C-O stretching, and peaks at 916.02 cm^{-1}, 854.31 cm^{-1}, 811.88 cm^{-1}, 723.18 cm^{-1} which represent C–C stretching. Furthermore, typical absorption peaks of vitamin E were observed at 1376.93 cm^{-1} (methyl groups), 1261.22 cm^{-1}, 1211.08 cm^{-1}, and 1085.73 cm^{-1} (C-O stretching and the phenol group) [27]. Figure 4(c) shows the spectrum of the 15% PLA/2% PMSQ scaffold. Similar peaks on the samples of the control group were observed at different wavelengths. The peak at 1747.19 cm^{-1} presents C = O stretching and other peaks at 1452.14 cm^{-1}, 1382.71 cm^{-1}, 1359.57 cm^{-1}, and 1268.93 cm^{-1} represent C-H bonding. The peaks at 1180.22 cm^{-1}, 1079.94 cm^{-1}, and 1039.44 cm^{-1} are related to C-O stretching. There were peaks at 863.95 cm^{-1}, 765.60 cm^{-1}, and 703.89 cm^{-1} which are correlated to C–C stretching.

3.4 Mechanical properties of the scaffolds

Table 1 shows the tensile testing results of each scaffold. The highest tensile strength value resulted in the 15% PLA scaffold (9.86 ± 2.19 MPa), whereas the value of the elongation at break was measured as 4.32 ± 0.61%. To find the optimum PMSQ concentration, tensile testing was performed on both scaffolds containing PMSQ alongside the 15% PLA scaffold. Compared to the 15% PLA scaffold, it can be said

Table 1 Tensile test results of each scaffold

Samples	Tensile stress (MPa)	Tensile strain (%)
15% PLA	9.86 ± 2.19	4.32 ± 0.61
15% PLA/1% PMSQ	6.93 ± 3.80	2.55 ± 2.37
15% PLA/2% PMSQ	7.27 ± 1.09	12.73 ± 15.29

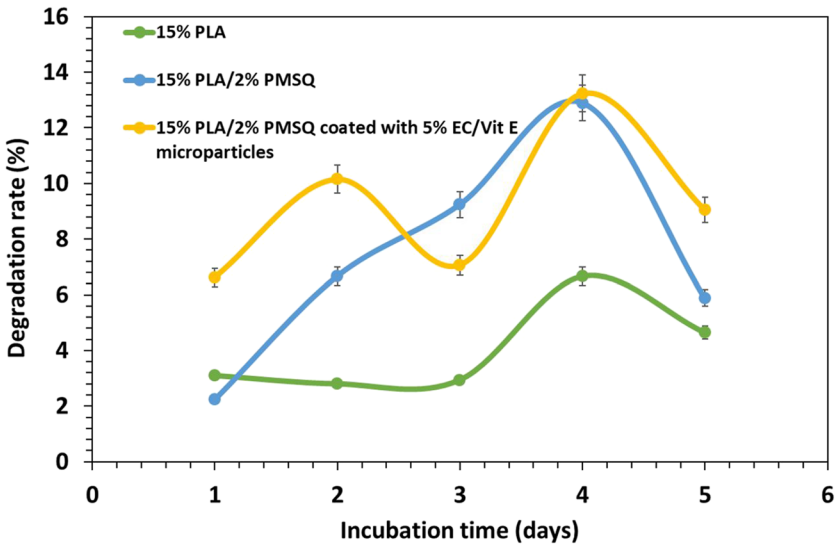

Fig. 5 The degradation behaviors of the scaffolds after 5 days of incubation

that the addition of PMSQ decreased the mechanical properties of the scaffold. When the PMSQ ratio increased to 2%, it resulted in higher mechanical properties than the 15% PLA/1% PMSQ scaffold. The tensile strength and elongation at break values of the 15% PLA/1% PMSQ were found to be 6.93 ± 3.80 MPa and 2.55 ± 2.37%, respectively. The addition of 2% PMSQ to 15% PLA scaffold increased the tensile strength again to a value of 7.27 ± 1.09 MPa and elongation at break value increased to a value of 12.73 ± 15.2%.

3.5 In vitro degradation test results

When structures are exposed to PBS, degradation happens when they dissolve over time [28]. Figure 5 demonstrates the degradation ratios of all scaffolds after incubation in PBS solution for various time periods. The 15% PLA/2% PMSQ scaffold coated with 5% EC/vitamin E microparticles showed the highest degradation rate at 13.24% on the fourth day of incubation. In the Fahimirad et al. study, they fabricated PCL/chitosan nanofibers and coated these nanofibers with curcumin-loaded chitosan nanoparticles. The degradation test performed in this study showed that electrospray chitosan/curcumin nanoparticles improved the degradation rate of PCL/chitosan nanofibers [29]. In comparison, the lowest degradation rate (6.66%) belonged to the 15% PLA scaffold. The hydrophobicity nature of both PLA and PMSQ

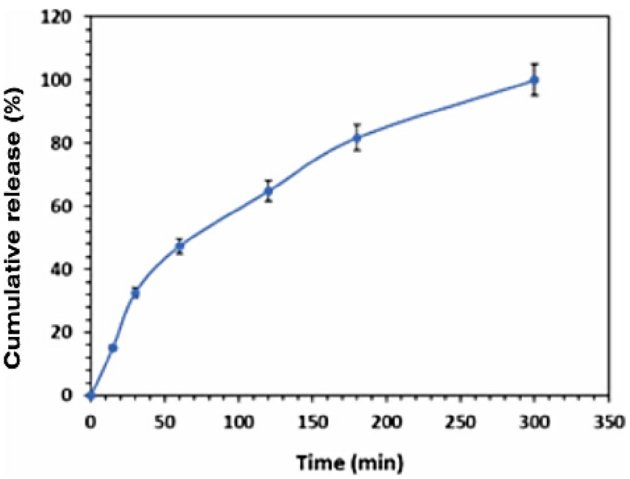

Fig. 6 The cumulative release graph of vitamin E released from 15% PLA/2% PMSQ scaffold

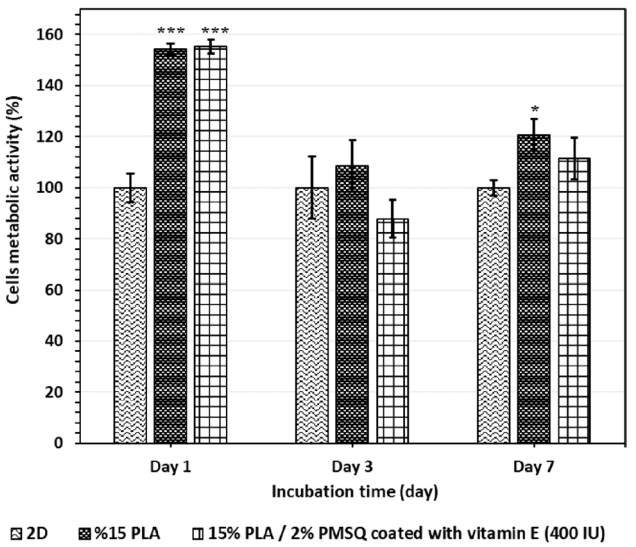

Fig. 7 MTT assay of the 3D-printed scaffolds after 1, 3, and 7 days of incubation time. One-way Analysis of Variance (ANOVA) Tukey–Kramer Multiple Comparisons Test Comparison to 2D $*p<0.05$, $***p<0.001$

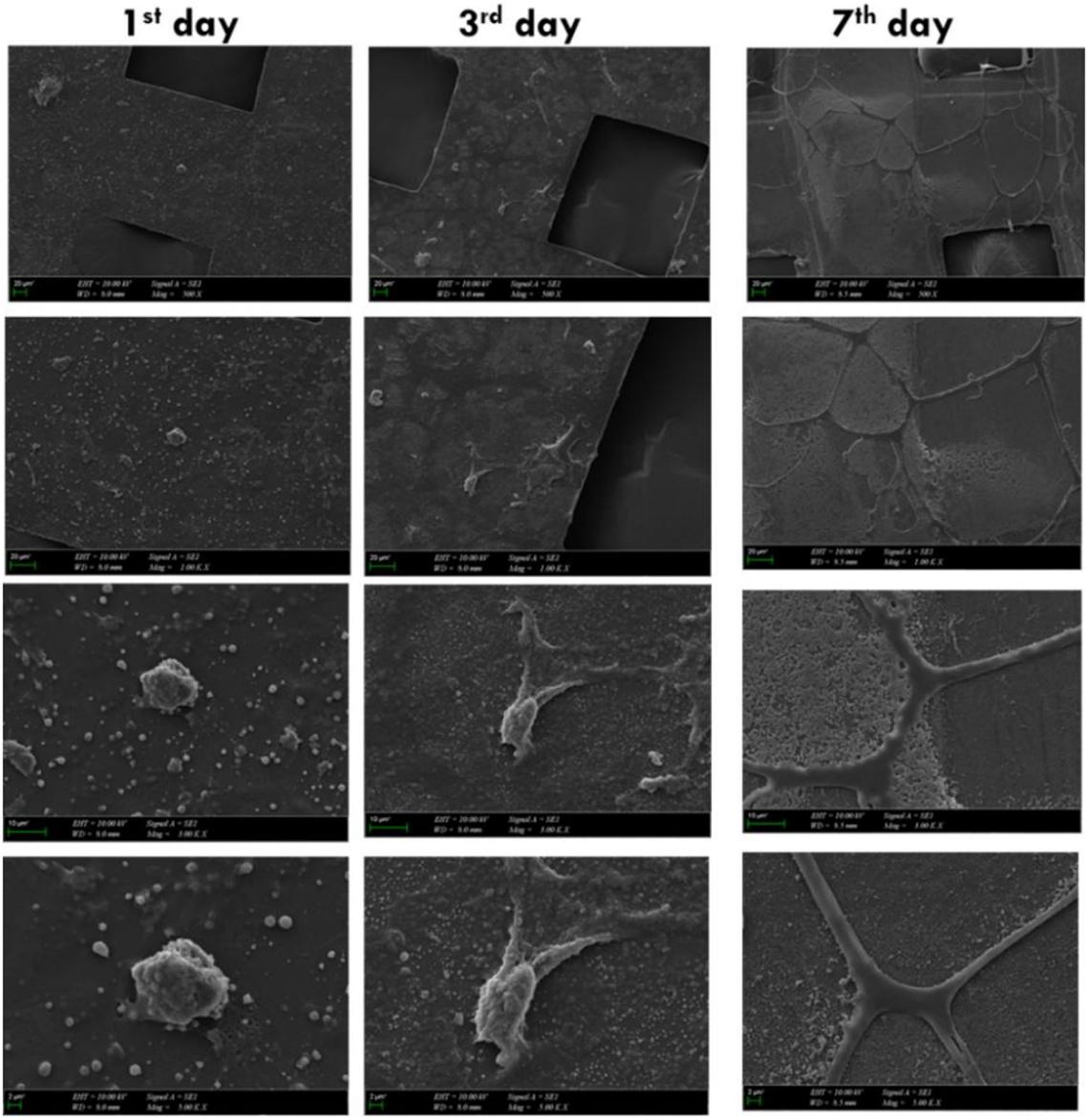

Fig. 8 SEM images of the cells on the 15% PLA/2% PMSQ scaffold coated with 5% EC/vitamin E over different days of incubation

affected their biodegradability properties. On the other hand, the addition of 2% PMSQ to 15% PLA increased the degradation ratios for all incubation times.

3.6 Vitamin E release from 15% PLA/2% PMSQ scaffolds

Figure 6 shows the cumulative release graph of the vitamin E from the scaffolds. The calibration curve was obtained using absolute ethanol mixed with vitamin E stock at different concentrations (0.2, 0.4, 0.6, 0.8, and 1.0 µg/mL) and the correlation coefficient (R^2) was calculated from the calibration curve. The absorbance plot of the vitamin E was determined at 235 nm. The results indicated that vitamin E was released from the 15% PLA/2% PMSQ scaffold within 5 h. According to the study carried out by Javier Pérez Quinones et. al., the release of vitamin E was completed in 7 h, which is similar to our study [30]. Therefore, it is possible to suggest that the release of vitamin E showed the same behavior as the literature.

3.7 MTT assay

MTT assay was used to obtain the biocompatibility properties of the scaffolds cultured with fibroblast cells for 1, 3, and 7 days. Figure 7 shows the viability of fibroblast cells when cultured with scaffolds after 1, 3, and 7 days of incubation compared to 2D (control group). After the

first day of incubation, the highest viability value was detected in the 15% PLA/2% PMSQ scaffold coated with 5% EC/vitamin E at 154.4 ± 12.23%. The 15% PLA had an 84.7 ± 7.87% viability value for the first day of incubation time. On the third day of incubation, the viability values of both scaffolds showed decreased values. The 15% PLA/2% PMSQ scaffold coated with vitamin E showed a viability value of 108.5 ± 10.16% and it was the highest compared to the viability of cells cultured with 15% PLA (71.1 ± 10.88%). On the seventh day of incubation, the viability value of 15% PLA/2% PMSQ scaffold coated with vitamin E increased and obtained as 120.8 ± 7.47% and was the highest compared to 15% PLA with a value of 101.4 ± 0.47%. According to the obtained results, both 15% PLA, and 15% PLA/2% PMSQ coated with vitamin E were biocompatible and not cytotoxic. 15% PLA/2% PMSQ scaffolds coated with vitamin E microparticles showed the highest cell growth and proliferation compared to others.

Figure 8 shows the SEM morphologies of the cells cultured with the 15% PLA/2% PMSQ scaffold coated with 5% EC/vitamin E microparticles after 1, 3, and 7 days of the incubation period. The cells were able to attach to the scaffolds and had a typical fibroblast morphological structure [31].

4 Conclusions

This research showed the ability to fabricate PLA/PMSQ-based scaffold coated with vitamin E microparticles using 3D printing technology and an electrospray method. The mechanical, thermal, chemical, morphological, and biological properties of the PLA/PMSQ scaffolds were examined. The biocompatibility results proved that scaffolds were not cytotoxic and biocompatible with fibroblast cells, it showed better viability results when coated with EC/vitamin E microparticles. SEM analysis showed the homogeneous morphology of the 3D scaffolds. The tensile test results showed that 15% PLA/2% PMSQ scaffolds had tensile strength slightly lower than 15% PLA scaffolds. According to results, it can be said that all combinations may have potential to be used in wound dressing applications.

Acknowledgements The authors receive no financial support for this research from any organization.

Data availability The raw data will be made available upon request.

Declarations

Conflict of interest The authors declare no conflict of interest.

References

1. Y. Liang, J. He, B. Guo, Functional hydrogels as wound dressing to enhance wound healing. ACS Nano **15**(8), 12687–12722 (2021)
2. Y. Yang, Y. Liang, J. Chen, X. Duan, B. Guo, Mussel-inspired adhesive antioxidant antibacterial hemostatic composite hydrogel wound dressing via photo-polymerization for infected skin wound healing. Bioact. Mater. **8**, 341–354 (2022)
3. R. Yu, H. Zhang, B. Guo, Conductive biomaterials as bioactive wound dressing for wound healing and skin tissue engineering. Nano-micro Lett. **14**(1), 1–46 (2022)
4. M. Hormozi, R. Assaei, M.B. Boroujeni, The effect of aloe vera on the expression of wound healing factors (TGFβ1 and bFGF) in mouse embryonic fibroblast cell: In vitro study. Biomed. Pharmacother. **88**, 610–616 (2017)
5. C.K. Sen, S. Khanna, G. Gordillo, D. Bagchi, M. Bagchi, S. Roy, Oxygen, oxidants, and antioxidants in wound healing: an emerging paradigm. Ann. N. Y. Acad. Sci. **957**(1), 239–249 (2002)
6. Y. Han, T. Sun, Y. Han, L. Lin, C. Liu, J. Liu, ... R. Tao, Human umbilical cord mesenchymal stem cells implantation accelerates cutaneous wound healing in diabetic rats via the Wnt signaling pathway. Eur. J. Med. Res. **24**(1), 1–9 (2019)
7. J. Qu, X. Zhao, Y. Liang, T. Zhang, P.X. Ma, B. Guo, Antibacterial adhesive injectable hydrogels with rapid self-healing, extensibility and compressibility as wound dressing for joints skin wound healing. Biomaterials **183**, 185–199 (2018)
8. Y. Liang, M. Li, Y. Yang, L. Qiao, H. Xu, B. Guo, pH/glucose dual responsive metformin release hydrogel dressings with adhesion and self-healing via dual-dynamic bonding for athletic diabetic foot wound healing. ACS Nano **16**(2), 3194–3207 (2022)
9. R. Dong, B. Guo, Smart wound dressings for wound healing. Nano Today **41**, 101290 (2021)
10. A.T. Hoang, L. Pallon, D. Liu, Y.V. Serdyuk, S.M. Gubanski, U.W. Gedde, Charge transport in LDPE nanocomposites Part I—Experimental approach. Polymers **8**(3), 87 (2016)
11. N. Hong, G.H. Yang, J. Lee, G. Kim, 3D bioprinting and its in vivo applications. J. Biomed. Mater. Res. B Appl. Biomater. **106**(1), 444–459 (2018)
12. M. Ayran, A.Y. Dirican, E. Saatcioglu, S. Ulag, A. Sahin, B. Aksu, A.M. Croitoru, D. Ficai, O. Gunduz, A. Ficai, 3D-Printed PCL scaffolds combined with juglone for skin tissue engineering. Bioengineering **9**(9), 427 (2022)
13. M.S. Izgordu, E.I. Uzgur, S. Ulag, A. Sahin, B. Karademir Yilmaz, B. Kilic, N. Ekren, F.N. Oktar, O. Gunduz, Investigation of 3D-printed polycaprolactone-/polyvinylpyrrolidone-based constructs. Cartilage **13**, 626S-635S (2021)
14. H. Karabulut, A. Dutta, Y. Moukbil, A.C. Akyol, S. Ulag, B. Aydin, R. Gulhan, Z. Us, D.M. Kalaskar, O. Gunduz, Fabrication of ethosuximide loaded alginate/polyethylene oxide scaffolds for epilepsy research using 3D-printing method. Front. Bioeng. Biotechnol., Sec. Biofabrication. **11**, 1244323 (2023)
15. M.K.I. Khan, A. Nazir, A.A. Maan, Electrospraying: a novel technique for efficient coating of foods. Food Eng. Rev. **9**(2), 112–119 (2017)
16. M. Pokorný, J. Klemeš, A. Kotzianová, T. Kohoutek, V. Velebný, Increased thickness uniformity of large-area nanofibrous layers by electrodynamic spinning. AIP Adv. **7**(10), 105214 (2017)
17. K.I. Deniz, S. Ulag, O. Gunduz, Investigation of the properties of encapsulated hydrophilic and hydrophobic drugs in whey protein microparticles. Mater. Lett. **324**, 132664 (2022)
18. E. Altan, Y. Karacelebi, E. Saatcioglu, S. Ulag, A. Sahin, B. Aksu, A.M. Croitoru, C.I. Codrea, D. Ficai, O. Gunduz, A. Ficai, Fabrication of Electrospun Juglans regia (Juglone) loaded Poly(lactic

acid) scaffolds as a potential wound dressing material. Polymers **14**(10), 1971 (2022)
19. A. Dingler, R.P. Blum, H. Niehus, R.H. Muller, S. Gohla, Solid lipid nanoparticles (SLNTM/LipopearlsTM) a pharmaceutical and cosmetic carrier for the application of vitamin E in dermal products. J. Microencapsul. **16**(6), 751–767 (1999)
20. M. Otadi, F. Zabihi, Vitamin E microcapsulation by ethylcellulose through emulsion solvent evaporation technique; an operational condition study. World Appl. Sci. J. **14**, 20–25 (2011)
21. H. Karabulut, S. Ulag, B. Dalbayrak, E.D. Arisan, T. Taskin, M.M. Guncu, ... O. Gunduz, A novel approach for the fabrication of 3D-printed dental membrane scaffolds including antimicrobial pomegranate extract. Pharmaceutics, **15**(3), 737 (2023)
22. K. Hamad, M. Kaseem, H.W. Yang, F. Deri, Y.G. Ko, Properties and medical applications of polylactic acid: a review. Express Polym. Lett. **9**(5), 435–455 (2015)
23. A.M. Croitoru, Y. Karaçelebi, E. Saatcioglu, E. Altan, S. Ulag, H.K. Aydoğan, ... A. Ficai, Electrically triggered drug delivery from novel electrospun poly (lactic acid)/graphene oxide/quercetin fibrous scaffolds for wound dressing applications. Pharmaceutics **13**(7), 957 (2021)
24. Q.W. Fu, Y.P. Zi, W. Xu, R. Zhou, Z.Y. Cai, W.J. Zheng, ... Q.R. Qian, Electrospinning of calcium phosphate-poly (D, L-lactic acid) nanofibers for sustained release of water-soluble drug and fast mineralization. Int. J. Nanomedicine. **11**, 5087 (2016)
25. I. Fernández-Cervantes, M.A. Morales, R. Agustín-Serrano, M. Cardenas-García, P.V. Pérez-Luna, B.L. Arroyo-Reyes, A. Maldonado-García, Polylactic acid/sodium alginate/hydroxyapatite composite scaffolds with trabecular tissue morphology designed by a bone remodeling model using 3D printing. J. Mater. Sci. **54**(13), 9478–9496 (2019)
26. B. Sibeko, Y.E. Choonara, L.C. du Toit, G. Modi, D. Naidoo, R.A. Khan, ... V. Pillay, Composite polylactic-methacrylic acid copolymer nanoparticles for the delivery of methotrexate. J. Drug Deliv. (2012)
27. P. Bracco, V. Brunella, M. Zanetti, M.P. Luda, L. Costa, Stabilisation of ultra-high molecular weight polyethylene with vitamin E. Polym. Degrad. Stab. **92**(12), 2155–2162 (2007)
28. E. Ilhan, S. Ulag, A. Sahin, B. Karademir Yilmaz, N. Ekren, O. Kilic, M. Sengor, D.M. Kalaskar, F.N. Oktar, O. Gunduz, Fabrication of tissue-engineered tympanic membrane patches using 3D-Printing technology. J. Mech. Behav. Biomed. Mater. **114**, 104219 (2021)
29. S. Fahimirad, H. Abtahi, P. Satei, E. Ghaznavi-Rad, M. Moslehi, A. Ganji, Wound healing performance of PCL/chitosan based electrospun nanofiber electrosprayed with curcumin loaded chitosan nanoparticles. Carbohyd. Polym. **259**, 117640 (2021)
30. J.P. Quiñones, K.V. Gothelf, J. Kjems, C. Yang, A.M.H. Caballero, C. Schmidt, C.P. Covas, Self-assembled nanoparticles of modified-chitosan conjugates for the sustained release of dl-α-tocopherol. Carbohyd. Polym. **92**(1), 856–864 (2013)
31. V.L. Masci, A.R. Taddei, G. Gambellini, F. Giorgi, A.M. Fausto, Ultrastructural investigation on fibroblast interaction with collagen scaffold. J. Biomed. Mater. Res., Part A **104**(1), 272–282 (2016)